IET Microwaves, Antennas & Propagation

Research Article

ISSN 1751-8725
Received on 16th August 2018
Revised 28th January 2019
Accepted on 5th February 2019
E-First on 5th April 2019
doi: 10.1049/iet-map.2018.5671
www.ietdl.org

EM lens design using thin planar metasurfaces for high antenna gain and low SLL applications

Rao Shahid Aziz[1] ✉, Tae-Wan Kim[1], Jae-Seok Park[2], Young-Ho Ryu[2], Seong-Ook Park[1]
[1]Department of Electrical Engineering, Korea Advanced Institute of Science & Technology (KAIST), Daejeon 305-732, Republic of Korea
[2]Samsung Electronics Co. Ltd., Suwon, Republic of Korea
✉ *E-mail: rshahid@kaist.ac.kr*

Abstract: A novel electromagnetic (EM) lens with high gain, suppressed side-lobe level (SLL) and low profile is designed using thin planar metasurfaces. The proposed design consists of a source patch antenna and an EM lens based on two thin planar metasurfaces. The two thin metasurfaces with an air gap are placed at the focal distance *H* of about $\lambda/2.25$ above the source patch antenna. This configuration forms a thin planar lens in which the source patch antenna emitted quasi-spherical wave in order to transform into plane wave. The total size of source antenna and an EM lens is same. The miniaturised EM lens antenna faces high SLL, which can be reduced by maintaining the uniform transmission phase coefficient and tunable transmission amplitude coefficient of metasurface unit cells. By implementing this topology on metasurfaces, the SLL of the proposed EM lens can be reduced without affecting the boresight gain of source patch antenna. The measured results of the proposed EM lens achieve 7 dB gain enhancement at designed frequency (5.8 GHz) with the SLL suppression of −24 dB. The total volume of planar lens antenna is $1.17\lambda \times 1.17\lambda \times \lambda/2.25$ mm^3, which is very compact compared with other reported planar lens designs.

1 Introduction

The high-gain antenna has been paid a great deal of attention due to its increased transmission distance property and decreased power consumption [1]. For long-distance wireless communications, high-gain antenna plays a vital role, therefore, different methods have been proposed for gain enhancements such as arrays [2], reflectors [3], cavities [4], lenses [5–7] and leaky wave antennas [8, 9].

There are few key challenges in lens antenna design. The main challenge in lens antennas is requiring large size approximately four or five times of the wavelength, which is necessary to meet the optical criteria [10]. At lower microwave frequencies, the size of the lens is larger as compared with traditional monopole, dipole or patch antennas. Commonly lens antenna is implemented in front of horn antennas which act as a source antenna and it further increases the antenna volume and makes it bulky. Therefore, it is very challenging to reduce the volume of the lens antenna by designing a small aperture size of the lens with shorter focal distance between the lens and source antenna. Moreover, reducing these parameters will also affect the overall performance of the lens for high-gain and low side-lobe applications.

Among various metamaterials, the gradient refractive index (GRIN) metamaterial can be characterised with different unit cells by varying geometries and dimensions. In the literature, many methods to design lenses using GRIN have been proposed [7, 10–15]. For example, in [7] a three-dimensional (3D)-transformed microwave high directive Luneburg lens antenna is presented operating on the X-band (from 8 to 12 GHz. It achieves a gain of about 15.8 dB at centre frequency (10 GHz), and low side-lobe levels (SLL) of about −26 dB in *E* and *H* planes. Zhu *et al.* in [10] proposed small metasurfaces using GRIN lens for antenna gain enhancement. The antenna possesses a circular shape with a diameter 1λ and achieves 5.5 dBi gain at 4.5 GHz. The proposed antenna has operating bandwidth from 4.4 to 4.65 GHz. A 3D source patch antenna comprised of 13 periodic vertical dielectric layers has been proposed to achieve high gain in [11]. Using this method, boresight gain has been improved up to 11.9 dB at 8.5 GHz. The overall volume of the antenna is about $1.7\lambda \times 1.6\lambda \times 1.7\lambda$ mm^3. The proposed antenna has 8–9 GHz operating bandwidth. In [12], a 3D lens using GRIN metamaterials is proposed, this antenna consists of multi-layer microstrip square-ring arrays. The proposed metamaterial GRIN lens antenna is operating at the X-band (from 8 to 12 GHz) and achieved gain is 6 dBi at 12 GHz. Similarly, a spherical lens with Luneburg index distribution is studied in [15] at the X-band and the Ku-band. The measured gain of the antenna at the X-band is from 17.3 (at 8.2) to 24 dB (at 19.8 GHz). The lens is fabricated using a polymer jetting rapid prototyping technique. These discussed planar lenses for high antenna gain applications require hard manufacturing process.

There are other significant researches presented to enhance the gain of the source antenna [16–23]. For example, in [16], Wenbo *et al.* proposed a novel design to reduce the radar cross-section and increase the gain of the patch antenna using partially reflecting surface (PRS). This design is composed of two metallic layers placed above a patch antenna. The results show that gain has been enhanced by about 6.5 dB at 11.5 GHz. The reflection coefficient is over − 3 dB from 11.25 to 11.7 GHz. In another work [17], Cheng *et al.* proposed a metasurface consisting of PRS with tunable phase cells from a Fabry–Perot resonance cavity, which enable a very high directive antenna. In addition to that varactor diodes were implemented on the metasurface cells for frequency tuning. The experimental results show that the antenna gain is increased about 7 dB by employing the metastructure, and its operation frequency can be dynamically tuned from 9.05 to 10 GHz. Cheng *et al.* proposed in [18] a low loss 6×6 reconfigurable circularly polarised transmitarray. The operating frequency band of the proposed design is 4.75–4.85 GHz. This transmitarray produces ± 45° beam steering at 4.8 GHz with a broadside measured gain of about 14.8 dBi high gain. It can be seen that even beam steering the gain of the proposed transmitarray remains same. Similarly, in [19] Cheng *et al.* proposed another 8×8 reconfigurable transmitarray with beam steering and polarisation manipulation capabilities at 5.4 GHz. The antenna gain is about 16.1 dBi at 5.4 GHz with the isolation between co- and cross-polarisations over 20 dB. Therefore, metasurface has many applications in wireless communication and is a good candidate to enhance the boresight gain of a source antenna.

In this paper, a low-profile electromagnetic (EM) lens designed using thin planar metasurfaces is proposed for high-gain antenna applications at 5.8 GHz. The total size of the proposed lens antenna is $1.17\lambda \times 1.17\lambda \times \lambda/2.25$ mm^3. The proposed EM lens is analysed

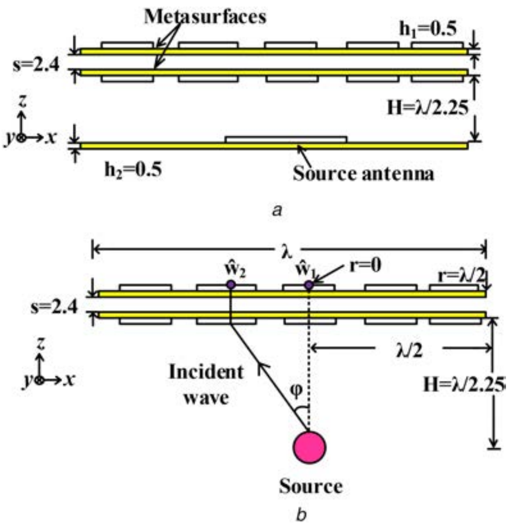

Fig. 1 *Side view of the proposed EM lens (all dimensions are in millimetres)*

Table 1 Parameters of the proposed EM lens design (all dimensions are in millimetres)

P	L	R_1	R_2	S	T_{total}	H
10.5	5,6,7	4.5	5	2.4	3.4	23
h_1	h_2	L_g	W_g	L_p	W_p	λ
0.5	0.5	60	60	16.62	20.26	51.7

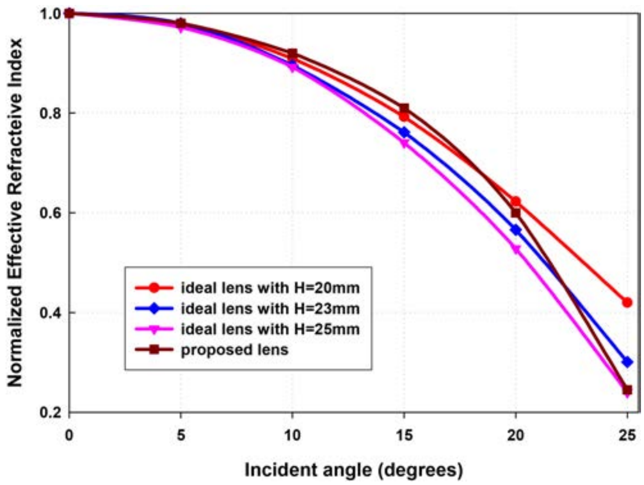

Fig. 2 *Normalised refractive index n(φ) of ideal lens and the proposed EM lens with varying focal distance H*

using GRIN standard function equations and designed using full wave EM simulation CST software. To validate the concept, a linearly polarised patch antenna is used as a source antenna. The proposed antenna successfully enhances the boresight gain of the source patch antenna. Meanwhile, the proposed EM lens suffers high SLL, which could further be optimised by only tapering the transmission amplitude (TA) of edge unit cells on metasurface, while maintaining the uniform transmission phase (TP). Finally, the designed EM lens with a source patch antenna has been fabricated and tested. The result shows that the thin metasurface-based EM lens can reduce main beamwidths (BWs) in radiation patterns and hence increase the boresight gain by 7 dB of the source patch antenna with suppressed SLL.

The organisation of this paper is as follows. Section 2 presents the working principle of the proposed EM lens in which the unit cell, the formation of EM lens and its focusing are discussed. In Section 3, the high-gain antenna consisting of linear polarised source patch antenna and the proposed EM lens are explained. Section 4 provides the design methodology of the proposed state of art. Section 5 gives the measured results of the proposed patch antenna with and without results in terms of its S parameters, radiation patterns and gain. Finally, a conclusion is drawn in Section 6.

2 EM lens using thin metasurfaces

2.1 Configuration of EM lens antenna

The configuration of EM lens is depicted in Fig. 1, comprises of two thin planar metasurfaces layers over the source patch antenna. The total volume of the proposed patch antenna with EM lens is width × length × height = 60 × 60 × 23 mm^3. The dielectric substrate is Taconic TLY-5z with relative permittivity, $\varepsilon_r = 2.2$, thickness, $t = 0.5$ mm and tangent loss, $\delta = 0.0009$. Two dielectrics metasurfaces are separated by an air gap of $s = 2.4$ mm. Table 1 shows the detailed parameters of the proposed EM lens. For high antenna gain applications, the EM lens is placed at a focal distance, H from a source patch antenna as shown in Fig. 1*a*. The source antenna emits linearly polarised EM waves along the z-axis which hits the thin planar metasurfaces with an incident angle φ. Fig. 1*b* shows the side view of the planar EM lens, which is placed at a focal distance H of about 23 mm (λ/2.25) from the source patch antenna. According to lens property in linear polarisation, the planar lens should contain the standard refractive index $n(r)$ of GRIN function along the x-axis from the centre point at $r = 0$ of the lens to the edge at $r = \lambda/2$ [10]. Therefore, from Fig. 1*b*, all EM waves radiated from the source, incident on EM lens surface and then passing through it, containing the same phase delay which can be added constructively. From [10, 24, 25], the two EM wave paths can be written as

$$\hat{w}_1 = \frac{H}{\lambda} + \frac{n(0) \times t}{\lambda} \tag{1}$$

$$\hat{w}_2 = \frac{\sqrt{H^2 + r^2}}{\lambda} + \frac{n(r) \times t}{\lambda} \tag{2}$$

Solving (1) and (2) for refractive index $n(r)$

$$n(r) = n(0) - \frac{\sqrt{H^2 + r^2} - H}{t} \tag{3}$$

In (3), the distance can be represented as $r = H \tan \varphi$ and $t = T_{\text{total}}$; therefore, (3) becomes [11]

$$n(\varphi) = n(0) - \frac{\sqrt{H^2 + (H \tan \varphi)^2} - H}{T_{\text{total}}} \tag{4}$$

The refractive index $n(\varphi)$ of (4) depends only on H, $T_{\text{total}} = t + s$. It does not consider relative permittivity (ε_r) of the dielectric metasurfaces and operating frequency, i.e. 5.8 GHz. For comparison between ideal GRIN lens, the normalised effective refractive index at $\varphi = 0°$ can be written as [11]

$$n(\varphi) = 1 - \frac{\sqrt{H^2 + (H \tan \varphi)^2} - H}{T_{\text{total}}} \tag{5}$$

From (5), the normalised effective refractive index $n(\varphi)$ of the ideal lens from varying $\varphi = 0$ to 25° having total thickness $T_{\text{total}} = 3.4$ mm and $H = 20$, 23, 25 mm can be calculated and graphically represented in Fig. 2.

2.2 Cross-shaped unit cell

To convert the incoming spherical EM waves from source antenna to plane wave, it should be ensured that the transmitted field from each unit cell of lens should be with an appropriate phase shift, and the TA coefficient must be nearly equal to one. The TP and amplitude coefficients play a vital role in the performance of EM lens unit cells. Therefore, for achieving high gain, low side-lobe and high efficiency; select a specific configuration of unit cell

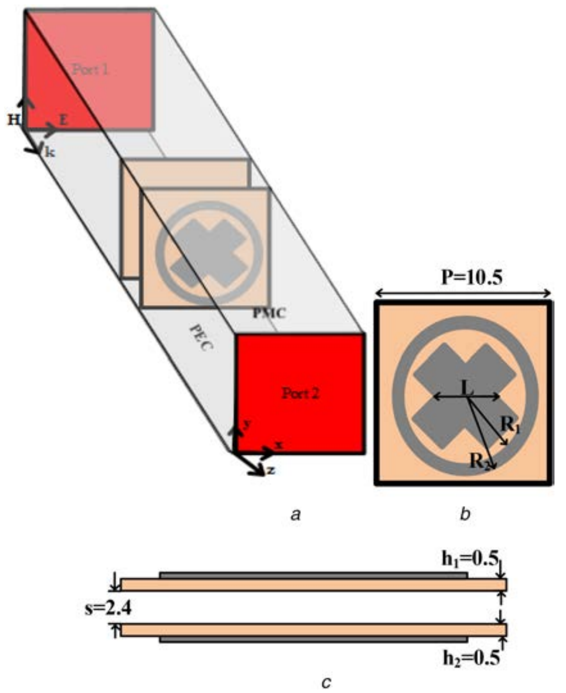

Fig. 3 *Model of the proposed EM lens using periodic boundary*
(a) Perspective view, ***(b)*** Front view, ***(c)*** Side view (all dimensions are in millimetres)

which provides wider phase range and a high amplitude of transmission coefficient.

To keep aforementioned points, single-layer unit cell is difficult to achieve the high TA coefficient; therefore, multiple layers can be a better solution to this problem. On the other hand, more than two layers can be bulky and hard for fabrication. Therefore, in the presented work, we have selected two thin layer substrates to avoid bulky profile. The performance of the proposed unit cell geometry is reasonable and applicable. The unit cell of the proposed EM lens is shown in Fig. 3. It is composed of two metallic layers and two intermediate dielectric layers with a gap of $s = 2.4$ mm. The dielectric layer (Taconic TLY-5) has a relative permittivity of 2.2 and a thickness of 0.5 mm. To avoid grating lobes, the size of the unit cell element should be <0.5λ (25.85 mm) [20]. Therefore, the configuration of the proposed unit cell with dimensions $P = 10.5$ mm is chosen. The parameter *'L'* is a variable, while the other parameters of lens remain fixed, i.e. P, R_1 and R_2. The unit cell is characterised in CST Microwave studio by applying periodic boundary conditions. From the computed S parameters of the unit cell, the refractive index $n(\varphi)$ of the unit cell is obtained using [26–28]

$$Z = \pm\sqrt{\frac{(1 + S_{11})^2 - S_{21}^2}{(1 - S_{11})^2 - S_{21}^2}} \tag{6}$$

$$e^{in(\varphi)k_oT_{\text{total}}} = X \pm i\sqrt{1 - X^2} \tag{7}$$

$$k_o = \frac{2\pi f}{c} \tag{8}$$

$$X = \frac{1}{\left[2S_{21}\left(1 - S_{11}^2 + S_{21}^2\right)\right]} \tag{9}$$

where $n(\varphi)$ is the effective refractive index; k_o is the wave number; T_{total} is the total thickness of the thin planar EM lens (including the air gap, s); f is the operating frequency, i.e. 5.8 GHz and c is the speed of light (3×10^8).

The signs in (6) and (7) are determined with the following two conditions:

$$\text{Re}[Z] \geq 0 \tag{10}$$

$$\text{Im}[n(\varphi)] \geq 0 \tag{11}$$

From [26], substituting (8) and (9) into (7) and considering the conditions of (9) and (10), the effective refractive index becomes

$$n(\varphi) = \frac{1}{k_oT_{\text{total}}}\left[\text{Re}\left\{\ln\left(e^{in(\varphi)k_oT_{\text{total}}}\right)\right\} - i\,\text{Im}\left\{\ln\left(e^{in(\varphi)k_oT_{\text{total}}}\right)\right\}\right] \tag{12}$$

Therefore, the characterisation of unit cell shown in Fig. 3 with the relative permittivity, $\varepsilon_r = 2.2$, and total thickness of the double-layer metasurfaces, $T_{\text{total}} = 3.4$ mm, the S parameters, effective refractive index $n(\varphi)$ for $\varphi = 0$ to 25° at the design frequency (5.8 GHz) can be calculated from (6) to (12).

The effective refractive index $n(\varphi)$ of the thin planar lens based on the characterisation of corresponding unit cells with the ideal lens can be computed for $\varphi = 0$ to 25° at 5.8 GHz, as shown in Fig. 2. It can be noted that the unit cell model of the proposed EM lens has a reasonable approximation compared with the ideal lens at $H = 23$ mm and φ<23°. At $H = 25$ mm, the unit cell model has an approximation at $\varphi = 24.8°$ that would lead to larger size. Similarly, at $H = 20$ mm the aperture size becomes smaller for antenna gain enhancement, which leads to inaccurate result. Therefore, for the proposed EM lens the best optimised approximation is $H = 23$ mm at about $\varphi = 22.58°$.

Fig. 4 shows the generation of cross-shaped cell, its simulated TA and phase coefficients by only varying its length L. In Fig. 4*a*, shows the transmission magnitude of two cascading unit cells. The resonating frequency of the transmission response depends on the length L of the cross-shaped unit cell. Varying length L of the unit cell from 5 to 7 mm, its resonating frequency is shifting which also leads to shift the TP. The proposed metasurface-based EM lens has very low profile; therefore, few discrete unit cells are required. The structure can be considered to be partially periodic as the phase responses of each unit cells are expected to be closer to the ideal case (infinite periodic structure) [21]. Hence, keeping the other parameters of a unit cell P, R_1, R_2 constant and only L is tuned different phase shift can be achieved on the lens metasurfaces. Fig. 4*b* shows the linear TP response at the designed frequency (5.8 GHz). By increasing the length L of cross shape from 5 to 7 mm, the phase shift is very small from 208° to 212° at 5.8 GHz.

2.3 Focusing EM lens design

Once the unit cell is characterised, the supercell can be designed. In our case, it consists of three cross-shaped unit cells to verify the ability to control the incident EM wave efficiently. This analysis of considering the supercell will be helpful for designing the complete EM lens to enhance the gain of the source antenna. The S parameter of the supercell shown in Fig. 5*a* is well-matched over designed frequency, and in Fig. 5*b* it can be seen that simulated E_x-field distribution in the *xoz*-plane indicate that it can focus the incident plane waves significantly.

The focusing property of a parabolic mirror is considered for designing a high directive antenna. Therefore, high-gain EM lens can be designed when the refractive phase distribution should obey the parabolic mirror profile, i.e. [29]

$$\Psi(x,\, y) = \frac{2\pi}{\lambda}\left(\sqrt{x^2 + y^2 + H^2} - H\right) + \Psi_0 \tag{13}$$

where H is the focal distance between the source and EM lens and Ψ is the phase shift.

The topology of complete EM lens is divided into a number of concentric zones populated with varying 'L' cross-shaped unit cells. Three concentric zones are utilised to develop the proposed EM lens geometry as shown in Figs. 6*a* and *b*. Total 5 × 5 unit cells satisfy the parabolic mirror profile from (13) in the *xoy*-plane. Figs. 6*c* and *d* show the simulated electric field distributions (E_x) at 5.8 GHz in *xoz* and *yoz* planes. Hence, it can be seen that the proposed lens configuration successfully focused the incoming EM waves along its paraxial direction.

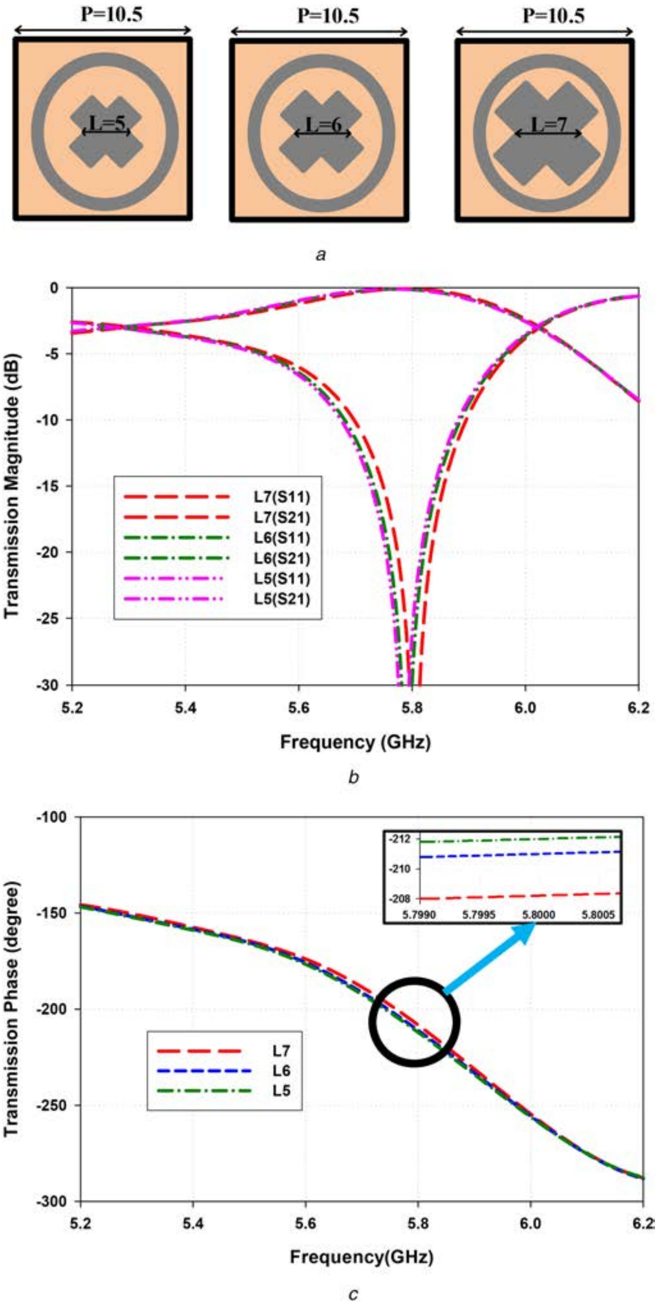

Fig. 4 *Cross-shaped unit cell*
(a) Generation of unit cell, ***(b)*** Transmission amplitude with different lengths *L*, ***(c)*** Transmission phase with different lengths *L*

3 Antenna design for high gain and low SLL applications

3.1 Isotropic source patch antenna

The configuration of a linear polarised source patch antenna is shown in Fig. 7. The length of the source patch antenna is W_p = 16.62 mm and the width is L_p = 20.26 mm and the total size of the substrate is $W_g \times L_g = 60 \times 60$ mm^2. The patch antenna is designed on Taconic TLY-z substrate with relative permittivity $\varepsilon_r = 2.2$, thickness and $t_{patch} = 0.5$ mm. The source patch antenna generates resonance at 5.8 GHz with 50 Ω feed line. Patch antenna is simulated and optimised using full wave EM simulation CST tool. Simulated and measured results of the source patch antenna will be discussed in detail in the next section.

3.2 Isotropic source patch antenna with EM lens

After the analysis of fine focusing of the proposed EM lens, a high-gain antenna at 5.8 GHz can be developed with thin planar metasurfaces and linearly polarised source patch antenna. From the

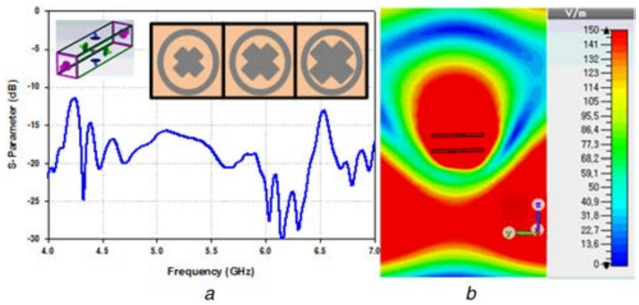

Fig. 5 *Supercell performance at 5.8 GHz*
(a) Reflection coefficient, ***(b)*** Simulated electric field distribution (*Ex*) in the *xoz*-plane

reciprocity of EM waves, the proposed EM lens significantly transforms the quasi-spherical wave emitted by the source patch antenna into quasi-plane wave. Therefore, double-layer metasurfaces have placed at a distance of $H = 23$ mm away from the source patch antenna along the $+z$ direction. Fig. 8 shows the E_x-field distribution of the source patch with and without

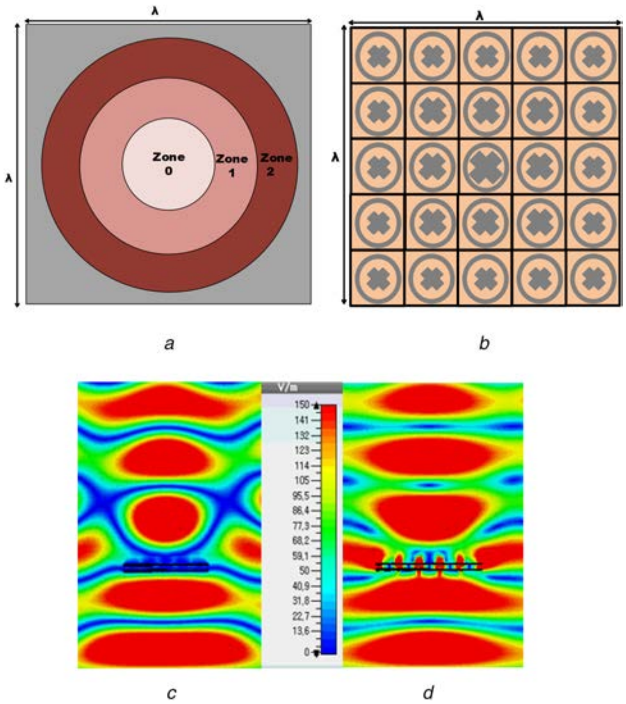

Fig. 6 *EM lens*
(a) Topology, ***(b)*** Geometry, and focusing effect at ***(c)*** *xoz*-plane and ***(d)*** *yoz*-plane using electric field (*Ex*)

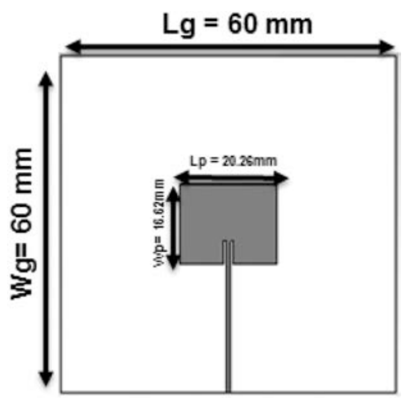

Fig. 7 *Configuration of a source patch antenna*

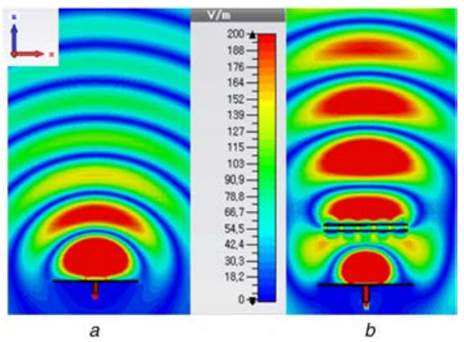

Fig. 8 *Simulated electric field distributions (Ex) at 5.8 GHz*
(a) Source patch antenna without EM lens at the *xoz*-plane, ***(b)*** Source patch antenna with EM lens at the *xoz*-plane

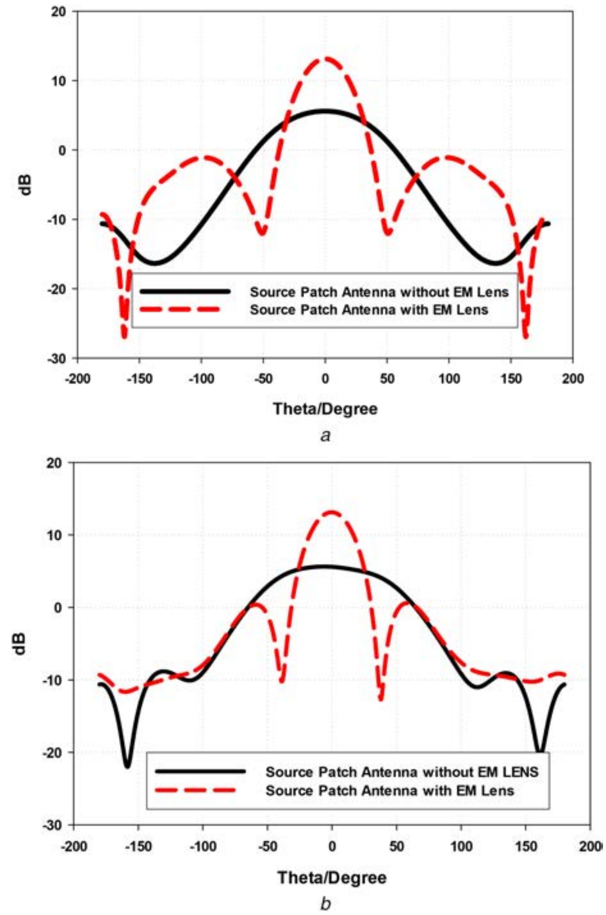

Fig. 9 *Simulated Cartesian far-field gain plots*
(a) *E*-plane patch with/without EM lens, ***(b)*** *H*-plane patch with/without EM lens

metasurfaces. It can be noted that the proposed EM lens successfully focused on the incident EM waves from the source patch antenna and transform the incoming quasi-spherical EM waves into plane wave as predicted theoretically in the *xoz*-plane.

Fig. 9 illustrates the simulated Cartesian gain plot of the source patch antenna with and without EM lens. It can be seen that the realised gain of the patch antenna at 5.8 GHz is enhanced from 5.1 to 12.1 dB which is about 7 dB. However, it can be noted that the SLL especially in the *E*-plane when source patch antenna with EM lens performing together they produce high SLL of about −14 dB in the *E*-plane. Therefore, in order to suppress SLL, later section addresses this issue in detail.

3.3 Suppressing side-lobe radiations of source patch antenna with EM lens

In planar metasurface lens design, the SLL is a great problem and it can be reduced by maintaining uniform TP and tunable TA coefficients. In this way, the *E*-field becomes tapered and the SLL can be reduced. On the other hand, reducing SLL will affect the gain of the antenna due to its intrinsic property. Therefore, in order to keep constant gain TA of the unit cell on the metasurfaces can be distributed intelligently. Initially, Taylor method [30] is adopted and the goal for SLL is set at −25 dB. The thin layer metasurface EM lens comprised of 5 × 5 arrays of unit cells; these unit cells are constructed to approximate an ideal Taylor TA distribution. Initially, the amplitude ratios are calculated from Taylor distributions: i.e. 0.8945, 0.9479, 0.9601, 1, 0.9601, 0.9479, and 0.8945. Further optimisation of correct TA and phase coefficients of EM lens unit cells will lead to suppressed SLL.

Implementing the aforementioned method to the presented EM lens geometry to achieve reduced SLL is a challenging task. Since in the proposed design, gain improvement is a major goal; therefore, in order to keep the antenna gain constant and simultaneously suppress SLL is very hard. This can be achieved by keeping TA of *zone* 0 and *zone* 1 uniform of the EM lens but tuning TA of *zone* 2. In other words, tuning the TPs of *zone* 0 and *zone* 1 of the EM lens but keeping the TP of *zone* 3 uniform.

To verify this scenario, the previously proposed topology of EM lens design will have to further optimise; especially *zone* 2 of the EM lens (edge unit cells, $L = 5$ mm; zone 2). *Zone* 0 and *zone* 1 unit cell configurations remain same; however, in *zone* 2 unit cells, two slots have been introduced in the outer circle of about 0.5 mm as depicted in Fig. 10*a*. The creation of slots on the modified unit

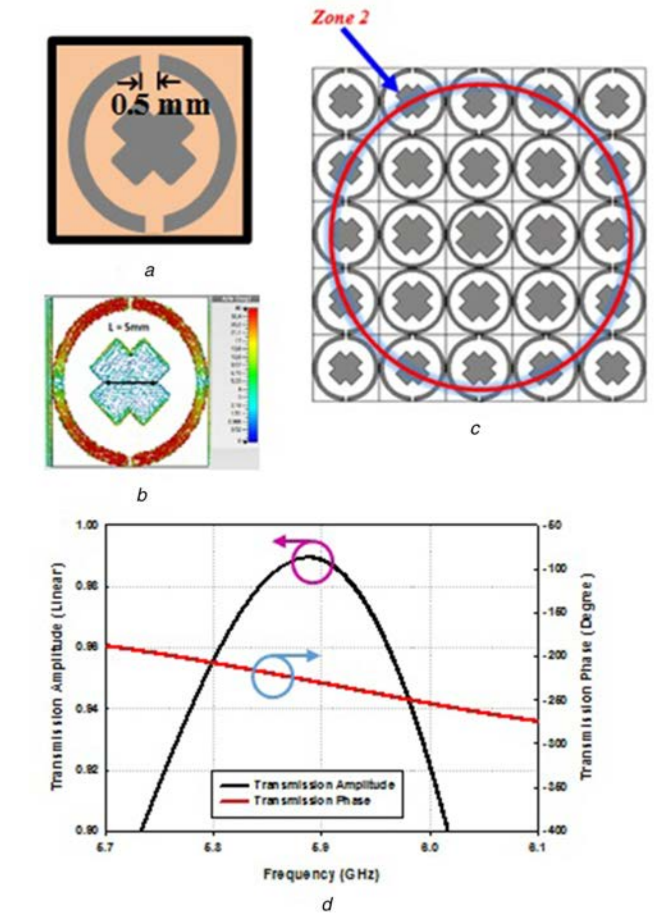

Fig. 10 *Modified unit cell*
(a) Configuration of unit cell with two slots, ***(b)*** Surface current distribution, ***(c)*** Topology of EM lens, ***(d)*** Transmission characteristics of modified unit cell

Table 2 Optimised parameters for TP and amplitude of EM lens

Unit cell	Slot	*L*, mm	TP	TA	RA	*A* = 1−TA^2−RA^2
1	no	7	−208	0.9875	0.00093	0.0248
2	no	6	−211	0.9842	0.0117	0.0312
3	yes	5	−212	0.9515	0.0131	0.0944

L is the length of the cross-shaped unit cell; TP is the transmission phase; TA is transmission amplitude; RA is reflection constant; and A is absorbance

cell produces capacitance and it helps to absorb the incoming EM waves. From current distribution in Fig. 10*b*, it can be seen that maximum current is flowing near the slot region and minimum current values are on the cross-shaped patch. This will lead to change the TA, while the phase remains same. The EM lens topology with the modified unit cell is depicted in Fig. 10*c*. It gives about 0.9515 value at 5.8 GHz as shown in Fig. 10*d* with TP=−212°.

After a number of recursive simulations, the obtained optimised parameters from three unit cells are mentioned in Table 2. This table also shows corresponding transmission characteristics, i.e. TA and TP and other important parameters such as reflection amplitude RA and absorbance A. These parameters are relatable and can be calculated as [31]

$$A = 1 - (\mathrm{TA})^2 - (\mathrm{RA})^2 \qquad (14)$$

Interestingly, it can be noted that the absorbance capability of zone 3 unit cells is higher compared with *zone* 0 and *zone* 1 cells. This method leads to obtain low SLL.

Fig. 11 shows the simulated Cartesian gain plot of a source patch antenna (*i*) without EM lens, (*ii*) with EM lens (high SLL) and (iii) with EM lens (optimised SLL). When the optimised unit

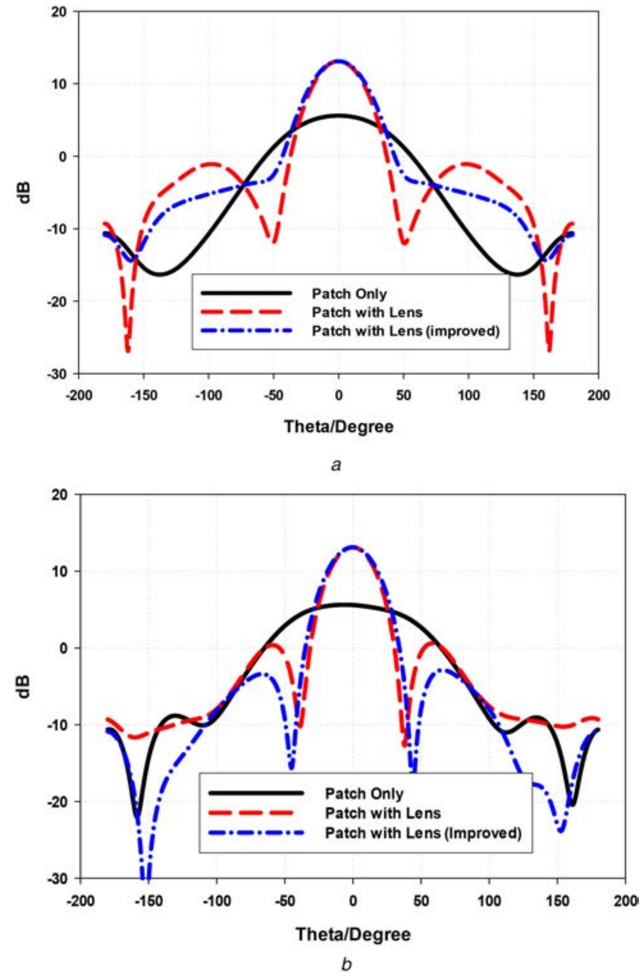

Fig. 11 *Simulated Cartesian far-field gain plots at*
(a) *E*-plane patch with/without EM lens, ***(b)*** *H*-plane patch with/without EM lens

cell in the *zone* 2 is employed on the EM lens, the SLL has been remarkably reduced from −14 to −24 dB in the *E*-plane. The gain of the antenna is about 12 dB. Similarly, in the *H*-plane, the SLL is reduced from −15 to −18 dB. The gain of the antenna is about 11.93 dB. Hence, the gain is slightly affected which can be negligible by modifying *zone* 2 unit cells. Therefore, the proposed EM lens geometry is an ideal candidate that possesses twin abilities, i.e. (*i*) enhancing the gain of the source antenna and (*ii*) suppressing the SLL.

3.4 EM lens design methodology

The methodology to design EM lens using metasurface can be summarised as follows:

i. Choose an operating frequency for EM lens.
ii. Choose a desired aperture size and shape for EM lens.
iii. Calculate the theoretical normalised refractive index $n(\varphi)$, using (5) to determine the appropriate focal distance *H*.
iv. Designing a suitable unit cell to resonate at the desired frequency and characterising it using (6)–(12).
v. Determine the phase-shifting property $\Psi(x,y)$ of designed unit cell by varying its geometrical configurations.
vi. Next step is the focusing of lens which can be determined from (13). At first a string of different phase unit cells called a supercell is generated. This supercell will verify the ability to control the incident EM wave efficiently (see Figs. 5*a* and *b*).
vii. Now, define the topology of EM lens by arranging its aperture into discrete concentric zones using selected different phase unit cells.
viii. Determining the feasibility of designed lens profile using (13). For example, this can be easily understood by analysing the electric field distributions as shown in Figs. 6*c* and *d*.

ix. To check the gain performance, select any source antenna (e.g. patch or horn). Place the designed EM lens at an optimised distance of H from (5), along a certain direction (see Figs. 1*a* and 2).

Furthermore, this state of art also addresses the solution to reduce the SLL while maintaining the high gain. This can be done by tuning the TA with uniform TP of specific unit cells. Complete process has already been discussed in the previous Section 3.3 in detail. Moreover, this methodology can be described with the help of a flowchart diagram as shown in Fig. 12.

4 Experimental results

The presented EM lens configuration and source patch antenna are fabricated. The lens prototype is comprised of two dielectric metasurfaces that are separated by air with a thickness of 2.4 mm, which is maintained by spacers on the edges of the dielectric substrates. The overall design (source patch antenna and EM lens) is fixed with stable plastics holders and screws mounted on the edges of the dielectric substrate. The metasurfaces and patch antenna are fabricated on a Taconic TLY-5z with relative permittivity 2.2, loss tangent of 0.0009 and substrate thickness 0.5 mm. The aperture size of the EM lens and patch antenna substrate size with screw holes are same, i.e. $70 \times 70\ \text{mm}^2$. The optimised focal length is 23 mm ($\lambda/2.25$) between source patch antenna and EM lens. The distance is maintained between source antenna and EM lens by plastic holders and screws. Fig. 13 shows the photograph of the EM lens and source patch antenna.

The measured and simulated impedance matching results of source patch antenna with and without EM lens are shown in Fig. 14. The source patch antenna is operated at 5.8 GHz. When the EM lens is attached at a distance of about 23 mm above the source patch antenna, the operating frequency slightly shifted to 5.805 GHz in the S parameter measurement plot. However, reasonable impedance matching of source patch antenna with and without EM lens is observed at about −30 dB.

Radiation patterns of the proposed thin planar lens antenna have been tested in an anechoic chamber. The simulated and measured radiation patterns of a source patch antenna with and without EM lens at 5.8 GHz are plotted in Fig. 15. From the experiment, the obtained maximum gains of the simulated and measured patterns for the single source patch antenna are 5.1 and 5.02 dB, respectively. Similarly, the achieved maximum gains of the simulated and measured patterns for the source patch antenna with EM lens are 12.1 and 12.02 dB, respectively. From Fig. 15, it can be noted that the simulated and measured radiation patterns show reasonable agreement and 7 dB gain enhancement is noted from the measurement patterns.

Furthermore, from Fig. 15*a* it can be observed that the half-power BWs (HPBWs) for simulated and measured cases in the E-plane of the source patch antenna without EM lens are 95.5° and 93°, respectively. On the other hand, the source patch antenna with EM lens measured HPBWs are 32° and 30°, respectively. In the H-plane, from Fig. 15*b* shows that the simulated and measured HPBWs of the source patch antenna are 85.7° and 80°, respectively. However, source patch antenna with EM lens for simulated and measured cases, the HPBWs in the H-plane are 33.2° and 30.5°, respectively. Hence, reported plots show that the EM lens can remarkably reduce the HPBW in both E and H planes, which result in gain enhancement. Moreover, the SLL with lens has been improved from −14 to −24 and −12 to −18 dB in both E and H planes, respectively. Fig. 15 shows the maximum realised gain of source patch antenna with and without EM lens. In simulation, the source patch antenna with and without EM lens has realised gains 5.1 and 12.15 dB, respectively; thus the EM lens greatly increases the boresight gain by 7.05 dB at 5.8 GHz. While in the measurement case, the EM lens increases the gain from 5.02 to 12.02 dB by 7 dB at 5.805 GHz. It can be seen that the gain has been enhanced on the designed operating frequency range and both the simulation and measurement trends are reasonably well-matched as shown in Fig. 16.

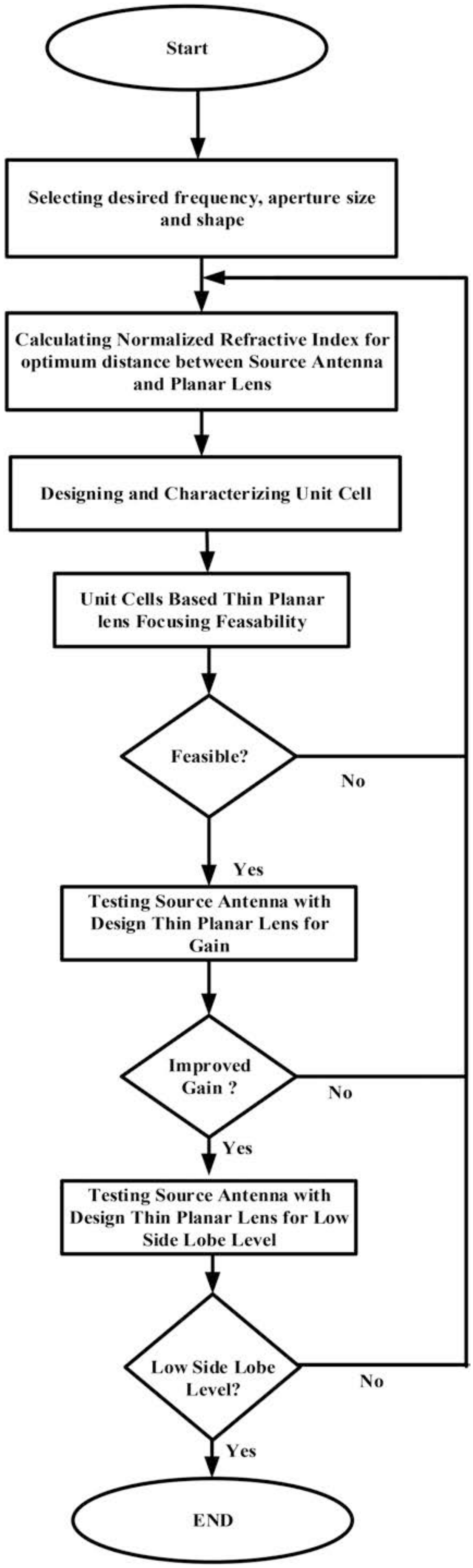

Fig. 12 *Flowchart for the proposed designed methodology of EM lens*

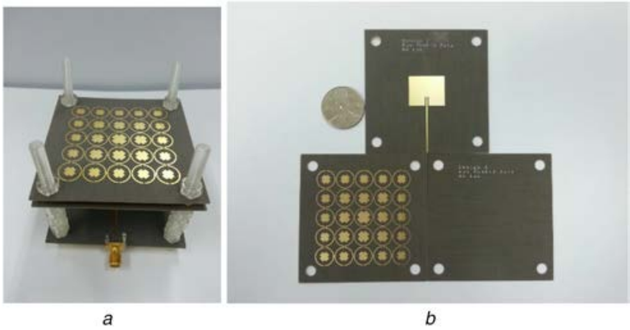

Fig. 13 *Photograph of a fabricated prototype of proposed antennas*
(a) Proposed source patch antenna loaded with EM lens, ***(b)*** Photograph of the lens and source patch antenna parts

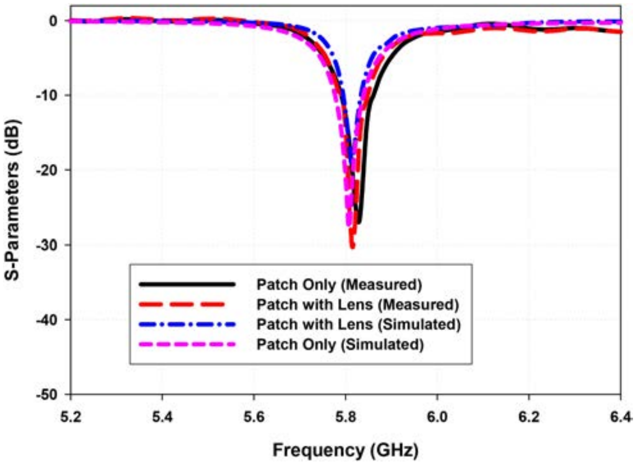

Fig. 14 *Simulated and measured S parameters of a source patch antenna with and without the EM lens*

Furthermore, antenna aperture efficiency can be calculated to characterise the performance of the proposed EM lens antenna. Therefore, from [9, 22, 23]

$$G_{\max} = \left(\frac{4\pi}{\lambda_{\mathrm{o}}}\right) A_{\mathrm{eff}} E_{\mathrm{f}} \tag{15}$$

where A_{eff} is an effective aperture; $G_{\max}$ is the maximum gain; and E_{f} is the radiation efficiency. The aperture efficiency can be calculated by

$$e_{\mathrm{a}} = \frac{A_{\mathrm{eff}}}{A_{\mathrm{physical}}} \tag{16}$$

where A_{physical} is the physical aperture size, in our case 60×60 mm^2, excluding the supporting area. Therefore, from (15) and (16), the calculated patch antenna only aperture efficiency is about 28.45%, whereas calculated antenna aperture efficiency with EM lens is about 91.46%. Hence, the proposed surface aperture is highly efficient. The total antenna efficiency is about 90% at the designed frequency.

Finally, a comparison table has been made with other proposed GRIN lenses based on gain enhancement in Table 2. Therefore, from Table 3, it can be concluded that the proposed lens has a gain enhancement of 7 dB in a compact volume of $1.17\lambda \times 1.17\lambda \times \lambda/2.25$ mm^3 as compared with other reported planar lenses.

4.1 Conclusions

A linear polarised source patch antenna with a thin planar double-layer metasurface-based EM lens has been presented for high antenna gain and low SLL applications. The proposed planar EM lens consists of two thin dielectric layers. Initially, the unit cell has been characterised and then the feasibility of the EM lens

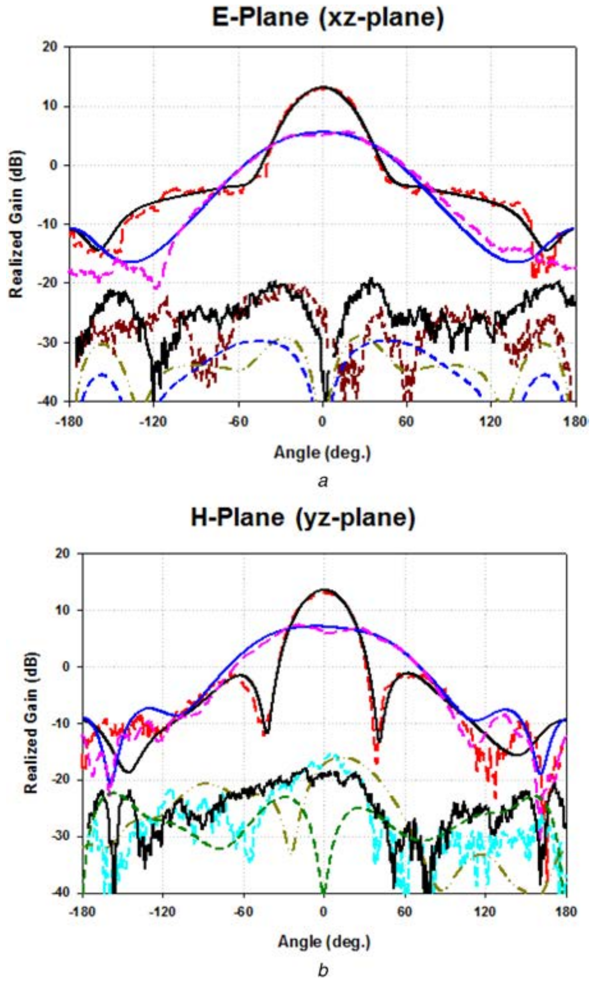

Fig. 15 *Measured and simulated co-polarised and cross-polarised radiation patterns for the source patch antenna with and without the EM lens*
(a) *E*-plane, ***(b)*** *H*-plane

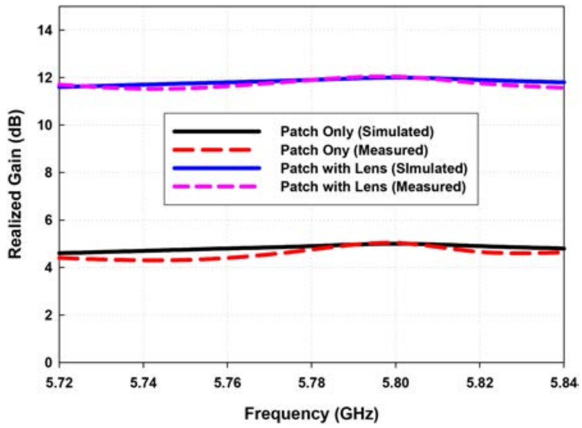

Fig. 16 *Trend of simulated and measured gains of source patch antenna with and without EM lens*

configuration based on unit cells is tested for good focusing performances. Finally, the proposed EM planar lens is placed with source patch antenna to verify the concept. The total occupied area of EM lens based on thin metasurfaces with source patch antenna is $1.17\lambda \times 1.17\lambda$ mm^2 (excluded area of plastic holders and screws on the edges) with a focal distance $H = \lambda/2.25$. A linearly polarised source patch antenna has been designed at 5.8 GHz. It has been shown that the proposed EM lens geometry can enhance a promising boresight gain of 7 dB. Moreover, SLL technique has been implemented in the metasurfaces by maintaining the uniform phase and tunable amplitude of edge unit cell to suppress the SLL

Table 3 Comparison of the proposed EM lens with other reported lenses

Reference	Operating bandwidth	Gain enhancement	Aperture size
[1]	5.65–5.87 GHz	2.3 dB at 5.75 GHz	$1.2\lambda \times 1.2\lambda \times 0.4\lambda$
[6]	3–7.5 GHz	12.5 dB at 5.5 GHz	$4.4\lambda \times 2.2\lambda \times 2.2\lambda$
[7]	X-band (8–12 GHz)	12.4 dB at 10 GHz	$3.3\lambda \times 3.3\lambda \times 3.2\lambda$
[9]	X-band	peak gain at 9.9 GHz is 20.4 dB	$6.55\lambda \times 6.55\lambda \times \lambda$
[10]	4.4–4.65 GHz	5.5 dB at 4.5 GHz	$\lambda/2 \times \lambda/2 \times \lambda$
[11]	8–9 GHz	11.9 dB at 8.5 GHz	$1.7\lambda \times 1.6\lambda \times 1.7\lambda$
[12]	X-band	6 dBi at 12 GHz	$1.6\lambda \times 1.6\lambda \times \lambda$
[15]	X-band/Ku-band	17.3 dB (at 8.2 GHz)/24 dB (at 19.8 GHz)	$4\lambda \times 4\lambda \times 4.8\lambda$
[32]	X-band	4.3 dB from 8 to 12 GHz	$2\lambda \times 2\lambda \times 1.35\lambda$
proposed	5.75–5.82	7 dB at 5.805 GHz	$1.17\lambda \times 1.17\lambda \times 0.44\lambda$

'λ' represents the operating frequency over which the gain is enhanced.

of source patch antenna. It significantly reduces the SLL up to − 24 dB. The proposed antenna with EM lens has experimentally demonstrated. It shows a gain of 12.02 dB at 5.805 GHz. The HPBWs are about 32° and 30° at *E* and *H* planes, respectively. The SLLs are < − 24 and − 18 dB at *E* and *H* planes, respectively. The EM lens and the source patch antenna are easily fabricated by the standard printed circuit board processing and integrated with other planar circuits.

5 Acknowledgment

This research was financially supported by the DMC R&D Centre of Samsung Electronics Co. Ltd. (G01170095).

6 References

[1] Kim, J.H., Ahn, C.H., Bang, J.K.: 'Antenna gain enhancement using a holey superstrate', *IEEE Trans. Antennas Propag.*, 2016, **64**, (3), pp. 1164–1167

[2] Miligan, T.A.: '*Modern antenna design*' (Wiley, Hobeken, NJ, USA, 2005, 2nd edn.)

[3] Cutler, C.C.: 'Parabolic-antenna design for microwaves', *Proc. IRE*, 1947, **35**, (11), pp. 1284–1294

[4] Vigueras, M.G., Gomez-Tornero, J.L., Goussetis, G.*, et al.*: 'Efficient synthesis of 1-D Fabry–Perot antennas with low sidelobe levels', *IEEE Antennas Wirel. Propag. Lett.*, 2012, **11**, pp. 869–872

[5] Xu, H.-X, Wang, G.-M, Cai, T.*, et al.*: 'Miniaturization of 3-D anistropic zero-refractive-index metamaterials with application to directive emissions', *IEEE Trans. Antennas. Propag.*, 2014, **62**, (6), pp. 3141–3149

[6] He-Xiu, X., Guang-Ming, W., Zui, T.*, et al.*: 'An octave-bandwidth half Maxwell fish-eye lens antenna using three-dimensional gradient-index fractal metamaterials', *IEEE Trans. Antennas Propag.*, 2014, **62**, (9), pp. 4823–4828

[7] Segura, C.M., Dyke, A., Dyke, H.*, et al.*: 'Flat Luneburg lens via transformation optics for directive antenna applications', *IEEE Trans. Antennas Propag.*, 2014, **62**, (4), pp. 1945–1953

[8] Monticone, F., Alu, A.: 'Leaky-wave theory, techniques and applications: from microwaves to visible frequencies', *Proc. IEEE*, 2015, **103**, (5), pp. 793–821

[9] Pfeiffer, C., Grbic, A.: 'Planar lens-antennas of subwavelength thickness: collimating leaky-waves with metasurfaces', *IEEE Trans. Antennas Propag.*, 2015, **63**, (7), pp. 3248–3253

[10] Zhu, H., Cheung, S.W., Yuk, T.I.: 'Enhancing antenna boresight gain using a small metasurface lens: reduction in half-power beamwidth', *IEEE Antennas Propag. Mag.*, 2016, **58**, (1), pp. 35–44

[11] Li, Q.L., Cheung, S.W., Wu, D.*, et al.*: 'Microwave lens using periodic dielectric sheets for antenna-gain enhancement', *IEEE Trans. Antennas Propag.*, 2017, **65**, (4), pp. 2068–2073

[12] Chen, X., Ma, H.F., Zou, X.Y.*, et al.*: 'Three dimensional broadband and high-directivity lens antenna made of metamaterials', *J. Appl. Phys.*, 2011, **110**, p. 044904

[13] Pfeiffer, C., Grbic, A.: 'Cascaded metasurfaces for complete phase and polarization control', *Appl. Phys. Lett.*, 2013, **102**, p. 231116

[14] Wan, X., Jiang, W.X., Ma, H.F.*, et al.*: 'A broadband transformation-optics metasurface lens', *Appl. Phys. Lett.*, 2014, **104**, p. 151601

[15] Liang, M., Ng, W.R., Chang, K.*, et al.*: 'A 3-D Luneburg lens antenna fabricated by polymer jetting rapid prototyping', *IEEE Trans. Antennas Propag.*, 2014, **62**, (4), pp. 1799–1807

[16] Wenbo, P., Cheng, H., Chen, P.*, et al.*: 'A low-RCS and high-gain partially reflecting surface antenna', *IEEE Trans. Antennas Propag.*, 2014, **62**, (2), pp. 945–949

[17] Cheng, H., Wenbo, P., Xiaoliang, M.*, et al.*: 'A frequency reconfigurable directive antenna with wideband low-RCS property', *IEEE Trans. Antennas Propag.*, 2016, **64**, (3), pp. 1173–1178

[18] Cheng, H., Wenbo, P., Xiangang, L.: 'Low-loss circularly polarized transmitarray for beam steering application', *IEEE Trans. Antennas Propag.*, 2016, **64**, (10), pp. 4471–4476

[19] Cheng, H., Wenbo, P., Xiaoliang, M.*, et al.*: 'Using reconfigurable transmitarray to achieve beam-steering and polarization manipulation applications', *IEEE Trans. Antennas Propag.*, 2015, **63**, (11), pp. 4801–4810

[20] Mei, J., Chen, N., Zhang, Y.*, et al.*: 'Metamaterial-based thin planar lens antenna for spatial beamforming and multibeam massive MIMO', *IEEE Trans. Antennas Propag.*, 2017, **65**, (2), pp. 464–472

[21] Mudar, A., Nader, B.: 'Wideband planar microwave lenses using sub-wavelength spatial phase shifters', *IEEE Trans. Antennas Propag.*, 2011, **59**, (12), pp. 4542–4552

[22] Amit, K., Mahesh, P., Shiban, K.: 'High-gain and high-aperture-efficiency cavity resonator antenna using metamaterial superstate', *IEEE Antennas Wirel. Propag. Lett.*, 2017, **16**, pp. 2388–2391

[23] Li, D., Szabo, Z., Qing, X.*, et al.*: 'A high gain antenna with an optimized metamaterial inspired superstrate', *IEEE Trans. Antennas Propag.*, 2012, **60**, (12), pp. 6018–6023

[24] Chen, X., Ma, H.F., Zou, X.Y.*, et al.*: 'Three-dimensional broadband and high-directivity lens antenna made of metamaterials' *J. Appl. Phys.*, 2011, **110**, (4), pp. 044904–044904-8

[25] Gagnon, N., Petosa, A., MsNamara, D.A.: 'Research and development on phase-shifting surfaces (PSSs)', *IEEE Antennas Propag. Mag.*, 2013, **55**, (2), pp. 29–48

[26] Chen, X., Grzegorczyk, T.M., Wu, B.I.*, et al.*: 'Robust method to retrieve the constitutive effective parameters of metamaterials', *Phys. Rev. E, Stat. Phys. Plasmas Fluids Relat. Interdiscip. Top.*, 2004, **70**, p. 016608

[27] Markos, P., Soukoulis, C.: 'Transmission properties and effective electromagnetic parameters of double negative metamaterials', *Opt. Express*, 2013, **11**, pp. 649–661

[28] Smith, D.R., Schultz, S., Markos, P.*, et al.*: 'Determination of effective permittivity and permeability of metamaterials from reflection and transmission coefficients', *Phys. Rev. B*, 2002, **65**, p. 195104

[29] Li, H., Wang, G., Xu, H.*, et al.*: 'X-band phase-gradient metasurface for high-gain lens antenna applications', *IEEE Trans. Antennas Propag.*, 2015, **63**, (11), pp. 5144–5149

[30] Wang, M., Huang, C., Pu, M.*, et al.*: 'Metamaterial assisted antenna array for reduction of side lobe level', *IEEE ICMMT*, 2012, **5**, pp. 1–3

[31] Wang, M., Huang, C., Pu, M.*, et al.*: 'Reducing side lobe level of antenna using frequency selective surface superstrate', *Microw. Opt. Technol. Lett.*, 2015, **57**, (8), pp. 1971–1975

[32] Meng, F.Y., Liu, R.-Z., Erni, D.*, et al.*: 'Automatic design of broadband gradient index metamaterial lens for gain enhancement of circularly polarized antenna', *Prog. Electromagn. Res.*, 2013, **141**, pp. 17–32